









# Human Cerebrospinal Fluid Monoclonal LGI1 Autoantibodies Increase Neuronal Excitability

Hans-Christian Kornau, PhD <sup>1,2</sup> Jakob Kreye, MD <sup>1,3,4</sup> Alexander Stumpf, PhD <sup>2</sup>  
Yuko Fukata, MD, PhD <sup>5,6</sup> Daniel Parthier, MSc <sup>2</sup> Rosanna P. Sammons, PhD,<sup>2</sup>  
Barbara Imbrosci, PhD,<sup>2</sup> Sarah Kurpjuweit <sup>1,3</sup> Alexander B. Kowski, MD,<sup>3</sup>  
Masaki Fukata, MD, PhD <sup>5,6</sup> Harald Prüss, MD <sup>1,3†</sup> and Dietmar Schmitz, MD<sup>1,2,7†</sup>

**Objective:** Leucine-rich glioma-inactivated 1 (LGI1) encephalitis is the second most common antibody-mediated encephalopathy, but insight into the intrathecal B-cell autoimmune response, including clonal relationships, isotype distribution, frequency, and pathogenic effects of single LGI1 antibodies, has remained limited.

**Methods:** We cloned, expressed, and tested antibodies from 90 antibody-secreting cells (ASCs) and B cells from the cerebrospinal fluid (CSF) of several patients with LGI1 encephalitis.

**Results:** Eighty-four percent of the ASCs and 21% of the memory B cells encoded LGI1-reactive antibodies, whereas reactivities to other brain epitopes were rare. All LGI1 antibodies were of IgG1, IgG2, or IgG4 isotype and had undergone affinity maturation. Seven of the overall 26 LGI1 antibodies efficiently blocked the interaction of LGI1 with its receptor ADAM22 in vitro, and their mean LGI1 signal on mouse brain sections was weak compared to the remaining, non-ADAM22-competing antibodies. Nevertheless, both types of LGI1 antibodies increased the intrinsic cellular excitability and glutamatergic synaptic transmission of hippocampal CA3 neurons in slice cultures.

**Interpretation:** Our data show that the patients' intrathecal B-cell autoimmune response is dominated by LGI1 antibodies and that LGI1 antibodies alone are sufficient to promote neuronal excitability, a basis of seizure generation. Fundamental differences in target specificity and antibody hypermutations compared to the CSF autoantibody repertoire in N-methyl-D-aspartate receptor encephalitis underline the clinical concept that autoimmune encephalitis are very distinct entities.

ANN NEUROL 2020;87:405–418

Limbic encephalitis associated with antibodies to leucine-rich glioma-inactivated 1 (LGI1)<sup>1,2</sup> is the second most common form of the growing number of autoimmune encephalopathies (AIEs) with

autoantibodies targeting central nervous system antigens.<sup>3–6</sup> LGI1 encephalitis is characterized by generalized and partial epileptic seizures, often as faciobrachial dystonic seizures (FBDS),<sup>7</sup> spatial

View this article online at [wileyonlinelibrary.com](https://onlinelibrary.wiley.com/doi/10.1002/ana.25666). DOI: 10.1002/ana.25666

Received Apr 2, 2019, and in revised form Dec 30, 2019. Accepted for publication Dec 30, 2019.

Address correspondence to Drs Kornau and Prüss, German Center for Neurodegenerative Diseases (DZNE) Berlin, c/o Charité–Universitätsmedizin Berlin, CharitéCrossOver (CCO), Charitéplatz 1, 10117 Berlin, Germany. E-mail: [hans-christian.kornau@dzne.de](mailto:hans-christian.kornau@dzne.de), [harald.pruess@dzne.de](mailto:harald.pruess@dzne.de)

<sup>†</sup>H.P. and D.S. contributed equally to this work.

From the <sup>1</sup>German Center for Neurodegenerative Diseases (DZNE) Berlin, Berlin, Germany; <sup>2</sup>Neuroscience Research Center, Cluster NeuroCure, Charité–Universitätsmedizin Berlin, Berlin, Germany; <sup>3</sup>Department of Neurology and Experimental Neurology, Charité–Universitätsmedizin Berlin, Berlin, Germany;

<sup>4</sup>Department of Pediatric Neurology, Charité–Universitätsmedizin Berlin, Berlin, Germany; <sup>5</sup>Division of Membrane Physiology, Department of Molecular and Cellular Physiology, National Institute for Physiological Sciences, National Institutes of Natural Sciences, Okazaki, Japan; <sup>6</sup>Department of Physiological Sciences, School of Life Science, SOKENDAI, Graduate University for Advanced Studies, Okazaki, Japan; and <sup>7</sup>Einstein Center for Neurosciences, Berlin, Germany

Additional supporting information can be found in the online version of this article.

disorientation, and amnesia, and it affects preferentially 50- to 70-year-old men. Epileptic activity could be detected in frontal cortex as well as hippocampus of patients,<sup>3</sup> and magnetic resonance imaging (MRI) studies revealed marked atrophy and impaired microstructural integrity of the hippocampus, correlating with cognitive impairment.<sup>8</sup> LGI1 antibodies are present in serum and cerebrospinal fluid (CSF) of patients, and a recent study suggested that an increased LGI1-IgG CSF index correlates with worse outcome.<sup>9</sup> Like many other autoimmune disorders, LGI1 encephalitis is associated with a defined genetic predisposition.<sup>10–13</sup>

LGI1 is secreted by neurons as a 60kDa protein containing leucine-rich repeat (LRR) and epitempin (EPTP) repeat domains. It forms protein complexes with ADAM22 and ADAM23 at excitatory synapses and may actually link these two transmembrane proteins across the synaptic cleft.<sup>14,15</sup> LGI1 affects the development of glutamatergic synapses via postsynaptic density proteins like PSD-95<sup>14,16</sup> and regulates neuronal excitability through axonal Kv1.1 potassium channel complexes.<sup>17</sup> Mutations in the *LGI1* gene cause autosomal dominant partial epilepsy with auditory features (ADPEAF). Targeted deletion of *Lgi1* in mice resulted in lethal myoclonic epileptic seizures.<sup>18–20</sup> CA3 neurons of *Lgi1*<sup>−/−</sup> hippocampal slice cultures exhibited an increased intrinsic neuronal excitability that may explain seizure generation.<sup>21</sup>

Acute application of IgG from sera of limbic encephalitis patients increased the release probability of mossy fibers and enhanced the excitability of CA3 neurons in hippocampal slices.<sup>22</sup> Furthermore, continuous intraventricular infusion of such IgG preparations into the CSF of mice enhanced glutamatergic neurotransmission by increasing presynaptic excitability in 2 pathways.<sup>23</sup> Injection of human CSF containing LGI1 antibodies into the dorsal hippocampus of mice increased both the probability of glutamate release from CA3 neurons and the amplitude of population spikes in the CA1 area following Schaffer collateral stimulation.<sup>24</sup> Although immunosuppression is effective in 50 to 80% of patients with LGI1 encephalitis,<sup>4</sup> detailed insight into the composition of the humoral autoimmune response to LGI1 in the CSF and the role of single LGI1 antibodies is missing. As exemplified by recent studies of N-methyl-D-aspartate (NMDA) receptor encephalitis, sequencing and expression of monoclonal antibodies from patient samples allow a deeper understanding of autoimmune encephalopathies.<sup>25,26</sup> Here, we amplified and cloned variable heavy and light chain sequences from CSF-derived antibody-secreting cells (ASCs) and B cells of 3 patients with LGI1 encephalitis. We expressed

85 monoclonal recombinant antibodies and characterized their reactivities and antigen-binding sites. Furthermore, we explored the effects of single recombinant LGI1 antibodies on the intrinsic excitability of neurons and on glutamatergic synaptic transmission.

## Materials and Methods

### Mammalian Expression Constructs

The cDNAs for amino acids 1 to 558 of human LGI1 (NM\_005097.3), for amino acids 1 to 545 of human LGI2 (NM\_018176.3), and for amino acids 1 to 400 of human GluN1 (NM\_007327) were inserted into pFuse-rIgG-Fc1 (InvivoGen, San Diego, CA). The resulting plasmids encode human LGI1, human LGI2, and the aminoterminal domain (ATD) of human GluN1, respectively, fused to the Fc region of rabbit IgG (amino acids SKP-PGK) linked by amino acids GSSTMVRS. The chimeric constructs LRR1-EPTP2 and LRR2-EPTP1 encode rabbit Fc fusions of amino acids 1 to 223 of LGI1 and amino acids 218 to 545 of LGI2 or amino acids 1 to 217 of LGI2 and amino acids 224 to 557 of LGI1, respectively.

The cDNA for amino acids 32 to 727 of mouse ADAM22 N-terminally tagged with amino acids SWSQ was inserted into the cytomegalovirus expression vector for *IGL*<sup>27,28</sup> together with an adaptor encoding a C-terminal hemagglutinin (HA) epitope. The resulting plasmid encodes amino acids MGWSCIILFLVATA TGSWSQ, the extracellular region of mouse ADAM22, and the C-terminal amino acids ASYPYDVPDYA.

The cDNAs of rat LGI1 (AJ487517), mouse LGI2 (AY841361), rat LGI3 (NM\_001107277), and mouse ADAM22 (HM004095) were cloned by reverse transcription and polymerase chain reaction (PCR) amplification as previously described<sup>14,19</sup> and subcloned into cytomegalovirus promoter-driven vectors.

### Cloning and Expression of Immunoglobulins from Patient CSF Cells

All clinical investigations were conducted according to Declaration of Helsinki principles. Patients gave written informed consent prior to inclusion in the study, and analyses were approved by the Charité University Hospital Institutional Review Board.

Single cells were isolated from patients' CSF samples using fluorescence-activated cell sorting into 96-well PCR plates at the Flow Cytometry Core Facility of the German Rheumatism Research Center Berlin using the following gating strategy. T cells, monocytes, and NK cells as well as nonviable cells were excluded from preselected single lymphocytes by gating on CD3<sup>+</sup>/CD14<sup>−</sup>/CD16<sup>−</sup>/DAPI<sup>−</sup> events. From the remaining cells, we selected either CD138<sup>+</sup> ASCs or CD20<sup>+</sup> B cells. For B cells, CD27 expression was used to differentiate between CD20<sup>+</sup>/CD27<sup>+</sup> memory B cells (MBCs) and CD20<sup>+</sup>/CD27<sup>−</sup> non-memory B cells (NMBCs). The following antibodies were applied: anti-CD3-FITC (1:25; Miltenyi Biotec, Bergisch Gladbach, Germany; #130-098-162), anti-CD14-FITC (1:25, Miltenyi Biotec, #130-098-063), anti-CD16-FITC (1:25,

Miltenyi Biotec, #130-098-099), anti-CD20-PerCP-Vio700 (1:50, Miltenyi Biotec, #130-100-435), anti-CD27-APC-Vio770 (1:12.5, Miltenyi Biotec, #130-098-605), and anti-CD138-PE (1:50, Miltenyi, #130-098-122).

Cloning of antibody heavy and light chains from single CSF cells,<sup>25,27,29</sup> sequence analyses, and expression and purification of antibodies were performed essentially as previously described.<sup>25</sup> Sequencing was performed at LGC Genomics (Berlin, Germany). Antibodies were used for further analyses if they yielded >2µg human IgG/ml. For antibodies not reaching 2µg human IgG/ml, the production was repeated.

### Enzyme-Linked Immunosorbent Assay

96-well high-binding microplates (Greiner Bio-One International, Kremsmünster, Austria; #655061) coated with donkey anti-rabbit IgG (10µg/ml; Dianova, Hamburg, Germany; #711-005-152) were blocked and incubated with cell culture supernatants of HEK293 cells that expressed Fc fusion constructs. Cell culture supernatants containing monoclonal antibodies (mean ± standard deviation of human IgG concentrations: 10.7 ± 5.6µg/ml) or purified antibodies and horseradish peroxidase (HRP)-conjugated donkey anti-human IgG (1:5,000, Dianova, #709-035-149) were sequentially applied. After thorough washing, HRP activity was measured using 1-Step Ultra TMB-ELISA substrate (Thermo Fisher Scientific, Waltham, MA). The presence of immobilized antigens was confirmed by incubation with HRP-conjugated F(ab')<sub>2</sub> donkey anti-rabbit IgG (1:50,000, Dianova, #711-036-152). Human recombinant anti-GluN1 antibody 003-102<sup>25</sup> was used at 10ng/ml. Mouse monoclonal anti-LGI1 antibody, N283/7 (1:1,000), was obtained from the University of California, Davis/NIH NeuroMab Facility.

Competition between LGI1 antibodies and ADAM22 for LGI1 binding was evaluated by measuring binding of the HA-tagged soluble extracellular domain of ADAM22 (ADAMexHA) to LGI1 that had been preincubated with LGI1 antibodies at 1µg/ml for 15 minutes. Bound ADAMexHA was detected using mouse anti-HA.11 (1:2,000; BioLegend, San Diego, CA; #901515) and HRP-conjugated donkey anti-mouse IgG (1:5,000, Dianova, #715-035-150).

Background by HRP-conjugated detection antibody alone was subtracted from each value except for in Figure 1B.

### Immunohistochemistry of Mouse Brain Sections

For screening of recombinant monoclonal antibodies, unfixed 20µm sagittal mouse brain cryostat sections were thawed, washed with phosphate-buffered saline (PBS) and blocked (PBS supplemented with 2% bovine serum albumin [Carl Roth, Karlsruhe, Germany] and 5% normal goat serum [Abcam, Cambridge, MA]). Undiluted HEK293T cell supernatants containing human monoclonal antibodies were applied overnight at 4°C. After washing, sections were incubated with Alexa Fluor 488-conjugated goat anti-human IgG (1:1,000, Dianova, #109-545-003) in blocking solution. Sections were washed again and mounted with DAPI-containing Fluoroshield.

For costainings, sagittal mouse brain sections were fixed with 4% paraformaldehyde (PFA) and incubated sequentially with blocking solution containing additional 0.1% Triton X-100 (Chemsolute), with purified primary antibodies diluted to 5µg/ml and chicken anti-MAP2 (1:1,000, Thermo Fisher Scientific, #PA1-16751) and with Alexa Fluor 488-conjugated goat anti-human IgG (1:1,000) and Alexa Fluor 568-conjugated goat anti-chicken IgG (1:500; Invitrogen, Carlsbad, CA; #AB\_2534098).

### Immunohistochemistry of Wild-Type and *Lgi1*<sup>-/-</sup> Mouse Brain Sections

All animal studies described herein were reviewed and approved by the animal care committee of the National Institutes of Natural Sciences and were performed in accordance with its guidelines. Ten-micrometer cryostat sections from *Lgi1*<sup>-/-</sup> mice<sup>19</sup> and their littermate controls (wild-type; postnatal day [P]17) were fixed with acetone, rehydrated, blocked in PBS containing 10% donkey serum, and incubated with purified AB060-110 or AB060-203 (2µg/ml) and rabbit anti-Prox1 antibody (Abcam, ab11941; 1:500). Immunoreactions were visualized by Cy3-conjugated anti-human IgG and Alexa Fluor 488-conjugated anti-rabbit IgG secondary antibodies, respectively.

### Quantification of LGI1 Antibody Binding against Brain Tissue

For relative quantification of the binding strength of LGI1 antibodies, PFA-fixed mouse brain sections were stained with HEK293T cell supernatants containing 5µg/ml of monoclonal antibody and fluorescence intensity within the hippocampal CA3 region was quantified as described.<sup>30</sup> After medium background subtraction, fluorescence intensity values were put in relation to the maximum value.

### Cell-Based Binding Assay

COS7 cells expressing LGI family members and chimera on the cell surface were stained with purified human antibodies AB060-110 or AB060-203 (10µg/ml) and mouse FLAG M2 antibody (Sigma-Aldrich, St Louis, MO; #F3165, RRID: AB\_259529) as described.<sup>31</sup>

### Electrophysiological Recordings in Organotypic Slice Cultures

Animal husbandry and experimental intervention were performed according to the German animal welfare act and the European Council Directive 86/609/EEC regarding the protection of animals used for experimental and other scientific purposes. All animal maintenance was performed in accordance with the guidelines of local authorities (Berlin T 0100/03).

Hippocampal slice cultures were prepared from C57/Bl6N mice (P5–9) as described.<sup>32</sup> Antibodies were applied to the slices at 13 to 14 days in vitro at 100nM final concentration, and recordings were performed 24 to 48 hours later.

Prior to recording, slices were transferred to a submerged recording chamber (Luigs and Neumann, Ratingen, Germany) and perfused with oxygenated artificial CSF (ACSF; pH 7.4)

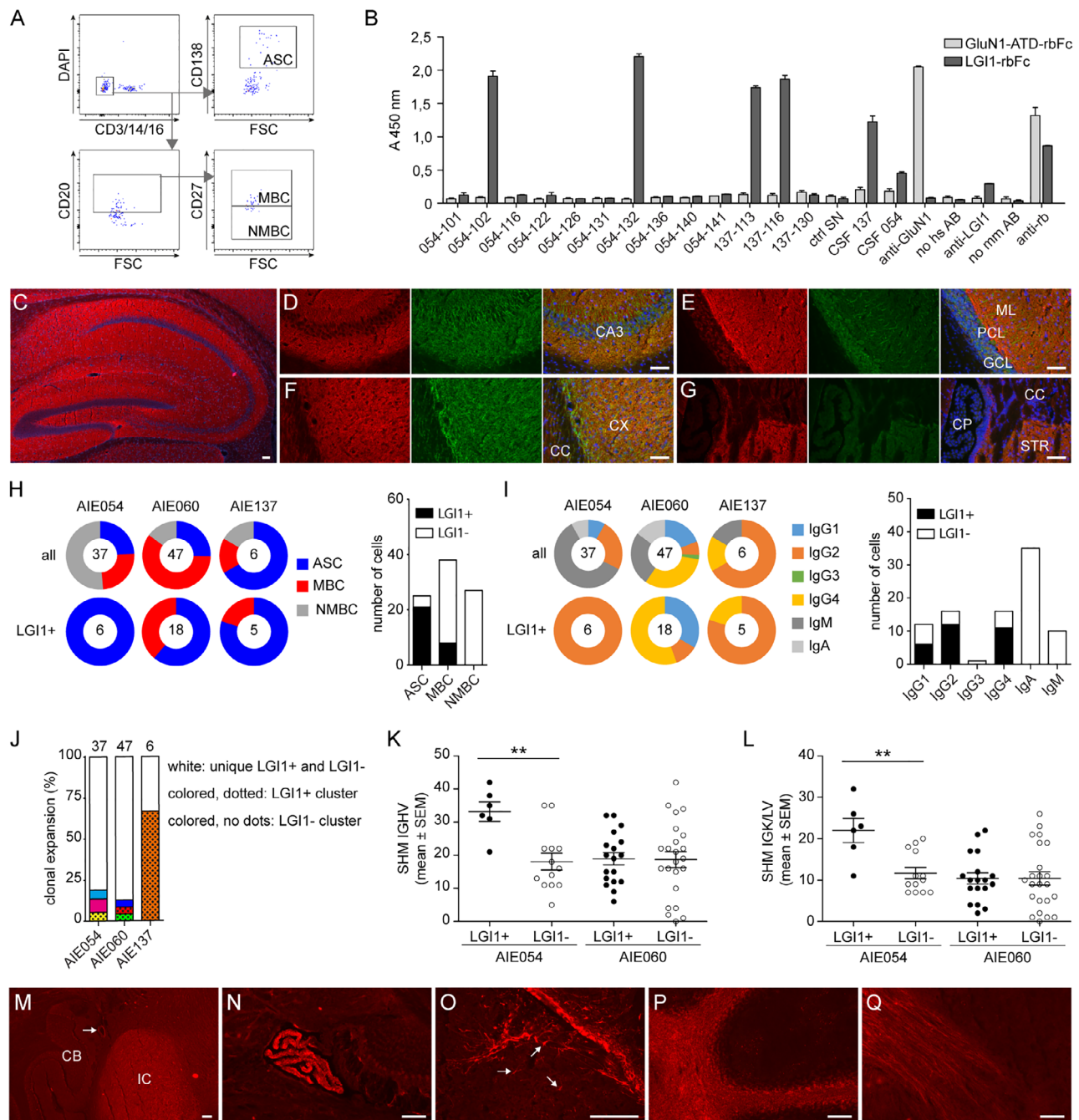


**FIGURE 1: An intrathecal B-cell immune response dominated by LGI1 antibodies.** (A) Isolation of single antibody-secreting cells (ASCs) as well as memory and nonmemory B cells (MBCs/NMBCs) from cerebrospinal fluid (CSF) of LGI1 encephalitis patients by flow cytometry. FSC = forward scatter. (B) To screen for LGI1 reactivity, cell culture supernatants of HEK293T cells expressing CSF cell-derived antibody cDNAs were applied to LGI1-Fc and to N-methyl-D-aspartate receptor subunit GluN1-ATD-Fc captured on an enzyme-linked immunosorbent assay plate. Example assay shows results for 13 supernatants as well as controls including CSF samples (diluted 1:5), human recombinant anti-GluN1, mouse anti-LGI1, and secondary antibodies to human, mouse, and rabbit IgG alone. Signals are shown as mean + standard deviation of 2 wells. (C–G) LGI1 (red signal) was detected by human recombinant antibody AB060-110 (5 µg/ml) in the hippocampal formation (C), the neuropil of hippocampal area CA3 (D), the molecular layer (ML) of the cerebellum (E), the cerebral cortex (F), and the striatum (G) on paraformaldehyde-fixed mouse brain sections. Costained neuronal MAP2 is shown in green, nuclei (DAPI) in blue. CC, corpus callosum; CP, choroid plexus; CX, cerebral cortex; GCL, granule cell layer; PCL, Purkinje cell layer; STR, striatum. (H) The majority of CSF-resident ASCs express LGI1 antibodies. Left: distribution of cellular phenotypes of all cells with successfully expressed antibodies and of LGI1-reactive cells (LGI1+) for each of the 3 patient samples. Variations in fluorescence-activated cell sorting settings/gate sizes account for variable fractions of NMBCs between patients. Right: total numbers of ASCs, MBCs, and NMBCs. AIE = autoimmune encephalitis. (I) LGI1-reactive antibodies were of the IgG1, IgG2 or IgG4 isotype. The distribution of isotypes is shown per patient sample (left) and in all cells (right). (J) Antibody sequence analyses indicated individual clusters of clonally expanded cells (Figure legend continues on next page.)

containing (in mM) NaCl (119), NaHCO<sub>3</sub> 26, glucose 10, KCl (2.5), NaH<sub>2</sub>PO<sub>4</sub> (1.25), MgCl<sub>2</sub> (4.0), and CaCl<sub>2</sub> (4.0) at room temperature, with a perfusion rate of 5ml/min. Excitability of the cells was measured in current clamp mode with a K-glucuronate-based intracellular solution containing (in mM) K-glucuronate (120), Hepes 20, KCl 3, NaCl 7, MgATP 4, NaGTP (0.3), and phosphocreatine 14, adjusted to pH 7.3 with KOH. Membrane potential values were corrected for liquid junction potential (−15mV). Membrane potential was manually adjusted to −75mV by continuous somatic current injection. Membrane response and action potential (AP) firing were measured by applying depolarizing current steps (duration = 1 second, increment = 40pA). For input–output curves, the number of APs was plotted with the injected current. The rheobase represents the minimal current eliciting at least 1 AP; AP threshold refers to the membrane potential at which an AP is triggered (5% of the maximal AP slope). The slope of the depolarizing ramp in current clamp mode was calculated in a 0.7-second time window at the current injection step before the rheobase. Cell capacitance and input resistance were detected in current clamp configuration by measuring the time constant  $\tau$  and the voltage deflection of a hyperpolarizing current pulse. For recordings with dendrotoxin-K (DTX-K; 100nM), either the slices were preincubated for at least 24 hours or acute wash-in of the toxin was performed.

To isolate  $\alpha$ -amino-3-hydroxy-5-methyl-4-isoxazolepropionic acid receptor (AMPA) miniature excitatory postsynaptic currents (mEPSCs), 1 $\mu$ M tetrodotoxin, 1 $\mu$ M SR95531 (gabazine), and 50 $\mu$ M D-AP5 were added to the ACSF. Slices were preincubated for 24 to 30 hours with antibodies or with DTX-K. Cells were recorded in voltage clamp configuration and were clamped to −70mV. mEPSC signals were detected automatically using IGOR Pro (WaveMetrics, Lake Oswego, OR) with the plugin Neuromatics and subsequently manually sorted by visual inspection. Cumulative distribution of mEPSC amplitude and interevent interval (IEI) were analyzed using an equal number of events per cell per condition to prevent overrepresentation of single neurons. Only cells where at least 10 IEIs could be detected were taken into account for the distribution. Kolmogorov–Smirnov test was performed to compare the distributions of individual conditions, and Bonferroni correction for multiple comparison was performed to adjust *p*-values.

Nonparametric 1-way analysis of variance (ANOVA) (Kruskal–Wallis) and Dunn multiple comparison test were performed to test significance in the different treatment conditions unless otherwise stated.

## Results

### CSF Cell Analysis Reveals a Polyclonal Humoral Immune Response with LGI1 as the Primary Target in the Brain

We set out to sequence and clone immunoglobulins from ASCs and B cells in the CSF of patients with LGI1 encephalitis following the strategy described previously for NMDA receptor encephalitis.<sup>25</sup> We used fluorescence-activated cell sorting to isolate NMBCs (CD20<sup>+</sup> CD27<sup>−</sup>), MBCs (CD20<sup>+</sup> CD27<sup>+</sup>), and ASCs (CD138<sup>+</sup>) from CSF of 3 patients fulfilling diagnostic criteria for LGI1 encephalitis with positive LGI1 autoantibodies (see Fig 1A). All 3 patients (AIE054, AIE060, and AIE137) showed characteristic symptoms of LGI1 encephalitis, with behavioral abnormalities, cognitive deficits, and seizures, and had mesiotemporal hyperintensities on T2/fluid-attenuated inversion recovery MRI (Table). At the time of CSF sampling, all patients had already received antiepileptic treatment and immunotherapy, which may have compromised the CSF B-cell response. The cell counts and protein levels from CSF were normal or slightly elevated, and only 1 of the patients had oligoclonal IgG bands present on routine laboratory tests.

RNA from single cells was reverse-transcribed, and the cDNAs encoding the variable regions for heavy and light chains were amplified and sequenced (Supplementary Table). The amplicons were cloned into IgG1 expression vectors.<sup>27,28</sup> The human antibodies were expressed in HEK293T cells, and the cell culture supernatants were tested for binding to a recombinant LGI1 fusion protein in an enzyme-linked immunosorbent assay (ELISA; see Fig 1B). Of 90 CSF cells, 29 encoded an LGI1-reactive antibody (AIE054: 6/9 ASCs, 0/9 MBCs, and 0/19

(colored). Sample sizes (number of cells) are given on top of the bars. (K, L) Human CSF LGI1 antibodies carry high numbers of somatic hypermutations (SHMs). The numbers of SHMs within the V gene segments of Ig heavy (IGH) chains (K) and of Ig kappa (IGK) or lambda (IGL) light chains (L) are plotted for each antibody generated from ASCs and MBCs of Patients AIE054 and AIE060 together with the mean  $\pm$  standard error of the mean (SEM). In AIE054, LGI1-reactive antibodies (LGI1+) contained higher numbers of SHMs than LGI1-negative (LGI1−) antibodies (unpaired *t* test, \*\**p* < 0.01; IGH: *p* = 0.0023; IGK/L: *p* = 0.0019, *n* = 6 and 13), whereas the numbers of SHMs were comparable in LGI1-reactive antibodies and LGI1-negative antibodies in AIE060 (IGH: *p* = 0.9381; IGK/L: *p* = 0.9991, *n* = 18 and 23). The number of antibodies generated from cells of AIE137 was too low to be included in this analysis. IGHV = immunoglobulin heavy chain V gene segment; IGK/LV = immunoglobulin kappa or lambda light chain V gene segment. (M–Q) Autoreactivities to unknown brain epitopes. Four of the human recombinant antibodies derived from LGI1 encephalitis patients' CSF cells showed clear reactivities to antigens other than LGI1 on unfixed mouse brain sections. (M) AB054-141 stains specifically the inferior colliculus (IC) within the mesencephalon and large blood vessels (arrow). CB, cerebellum. (N) AB060-108 is a weak LGI1-reactive antibody, but also highlights the choroid plexus. (O) 060-176HL is reactive to glial fibers (arrows) in different brain regions, most prominent around the ventricular system. (P, Q) 060-144 binds to fine tracks within the white matter, explicitly in the cerebellum (P) and the anterior commissure (Q). Scale bars = 100 $\mu$ m.





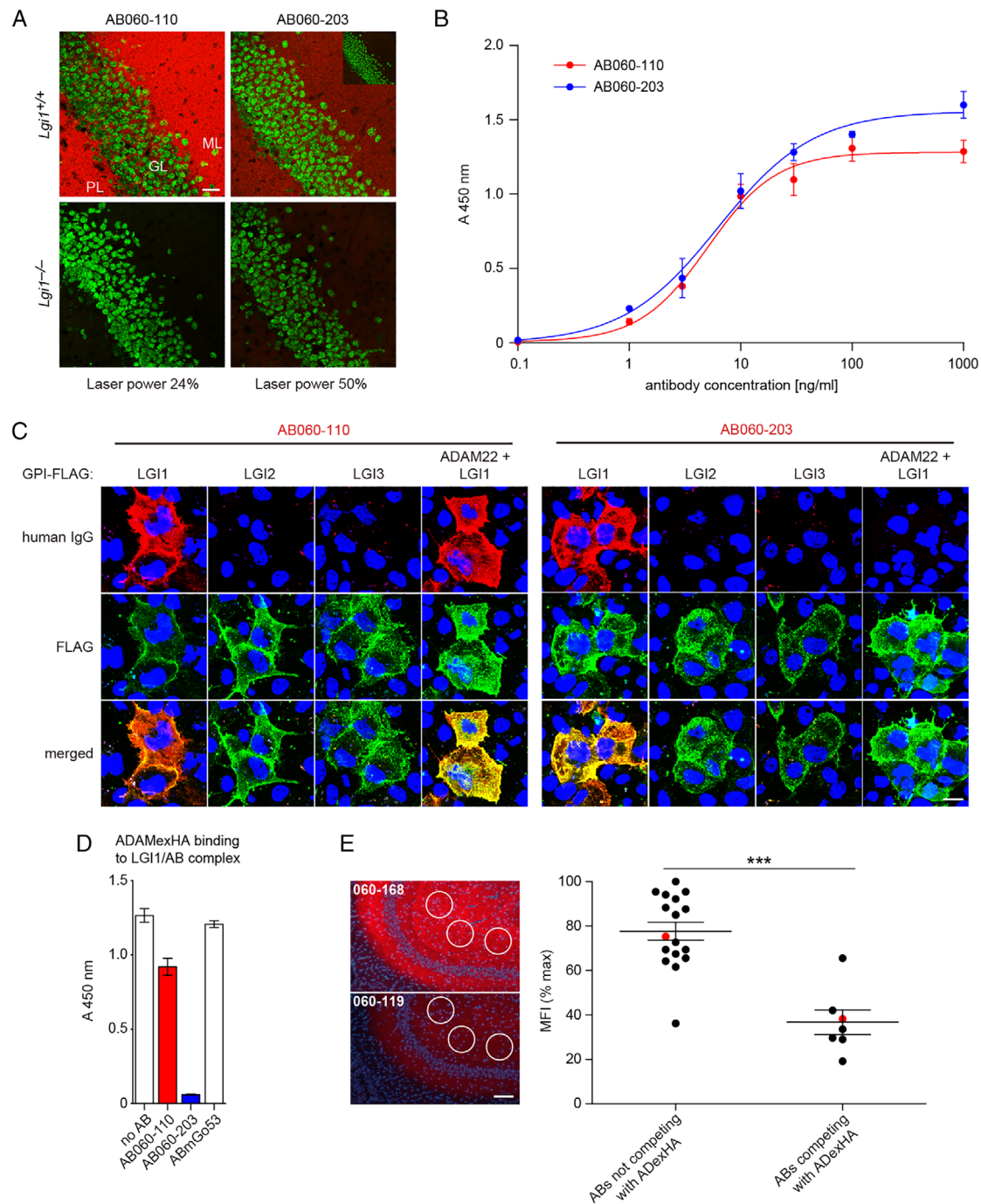


**FIGURE 3: Human monoclonal antibodies AB060-110 and AB060-203 specifically recognize LGI1, but differ in their access to native LGI1. (A)** Signals for both AB060-110 and AB060-203 are undetectable on *Lgi1*<sup>-/-</sup> sections. For AB060-203, laser power was increased from 24% to 50% during imaging, because the signal with AB060-203 was much weaker than the one with AB060-110 (*inset* shows the signal at 24% laser power). Dentate gyrus stainings of wild-type and *Lgi1*<sup>-/-</sup> sections are shown with human IgG and the granule cell marker Prox1 in red and green, respectively. GL = granule cell layer; ML = molecular layer; PL = polymorphic layer. Scale bar = 20  $\mu$ m. **(B)** Similar concentration-dependent binding of recombinant LGI1 by AB060-110 and AB060-203. Purified antibodies were applied at various concentrations to LGI1-Fc captured on an enzyme-linked immunosorbent assay (ELISA) plate. Signals are shown as mean  $\pm$  standard deviation (SD) from 3 wells. **(C)** Human monoclonal antibodies AB060-110 and AB060-203 differentially detect LGI1/ADAM22 complexes. Immunocytochemical analysis on COS7 cells expressing the proteins indicated in black on top of the images is shown. Bound human IgG and surface-expressed LGI-FLAG-GPI are shown in red and green, respectively. Left: AB060-110 specifically recognized LGI1 irrespective of coexpressed ADAM22. Right: AB060-203 specifically recognized recombinant LGI1. Coexpression of ADAM22 strongly reduced AB060-110 binding to LGI1. **(D)** AB060-203 efficiently blocked ADAM22 binding to LGI1. ELISA signals (mean  $\pm$  SD from 4 wells) indicate binding of the extracellular domain of ADAM22 (ADAM22) to LGI1-Fc after preincubation with purified monoclonal human (Figure legend continues on next page.)

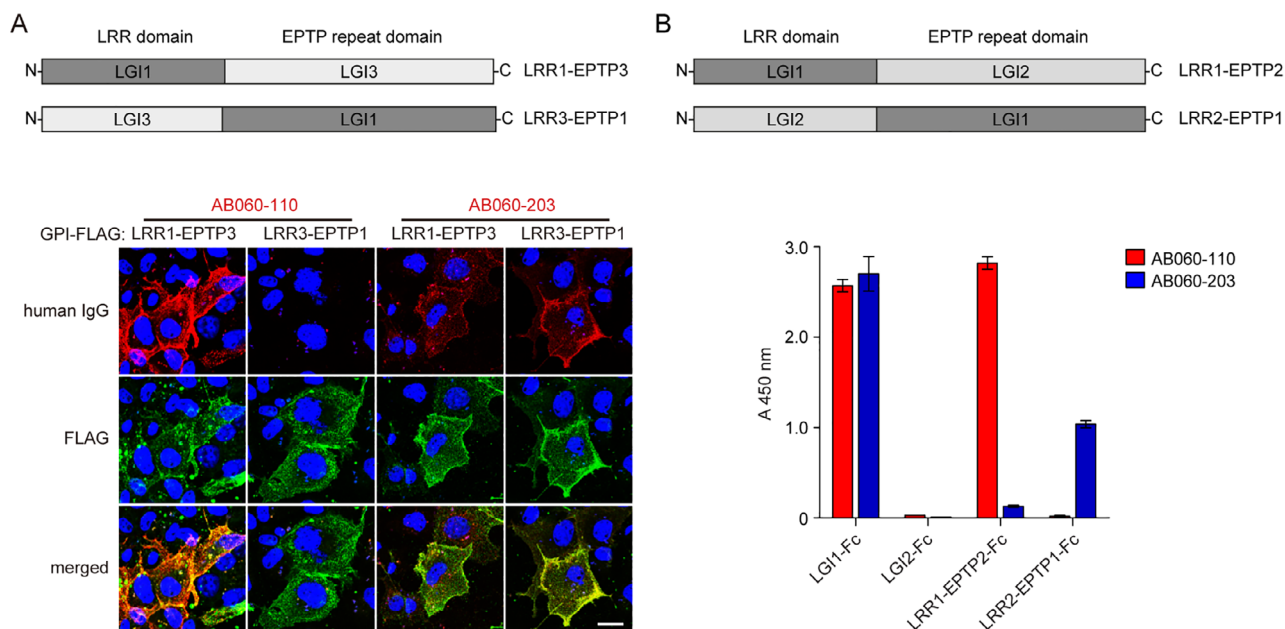


**FIGURE 4:** Human monoclonal antibodies AB060-110 and AB060-203 target different domains of LGI1. AB060-110 selectively recognized the leucine-rich repeat (LRR) domain of LGI1, whereas AB060-203 detected the epitempin (EPTP) repeat domain and weakly the LRR domain of LGI1. Schemes of chimeric constructs expressed to determine the target epitopes in LGI1 are shown on top. (A) COS7 cells expressing chimera of LGI1 and LGI3 were analyzed as in Figure 3C. Scale bar = 20 $\mu$ m. (B) Enzyme-linked immunosorbent assay signals of purified antibodies at 1 $\mu$ g/ml on LGI1-Fc, LGI2-Fc, or chimera thereof. Signals are shown as mean  $\pm$  SD from 3 wells.

extracellular domain of ADAM22 bound to immobilized LGI1 on 96-well plates. Pretreatment of LGI1 with seven of the monoclonal LGI1 antibodies reduced ADAM22-binding by >60% (Fig 2). Interestingly, each of the 3 patients' CSF samples contained ASCs expressing ADAM22-competing and ASCs expressing ADAM22-noncompeting antibodies, confirming the polyclonal nature of the LGI1 autoimmune response predicted earlier.<sup>31</sup> We selected and purified 2 LGI1 antibodies derived from ASCs of Patient AIE060, 1 interfering with the LGI1–ADAM22 interaction (AB060-203) and 1 that did not (AB060-110), and tested their LGI1 selectivity and ADAM competition in detail.

Immunohistochemistry on mouse brain sections of wild-type and *Lgi1* knockout mice proved that both of these antibodies recognize LGI1 selectively (Fig 3). However, although their concentration-dependent binding curves pointed to comparable binding efficiencies in the LGI1 ELISA, AB060-203, which efficiently competed with the soluble extracellular domain of ADAM22 for LGI1-binding, resulted in much weaker signals on mouse

brain sections than AB060-110. Immunocytochemistry on COS7 cells confirmed a selective recognition of surface-expressed LGI1, but not LGI2 or LGI3 by both AB060-110 and AB060-203. Interestingly, LGI1 detection by AB060-203, but not by AB060-110, was strongly reduced in COS7 cells coexpressing LGI1 and ADAM22. Thus, the LGI1 epitope recognized by AB060-203 can be masked by ADAM22. LGI1-binding by AB060-203 may be blocked by ADAM22 in vivo, and this may account for the reduced signals of AB060-203 against native LGI1. To test whether blockade of ADAM22-binding to LGI1 in the ELISA (see Fig 2) correlated with a reduced access to endogenous LGI1 in the brain in general, we determined the immunohistochemistry staining signal of all monoclonal LGI1 antibodies on mouse brain sections. Although the range of signals was wide, the group of antibodies that had reduced ADAM22-binding by >60% in the ELISA (see Fig 2) resulted in lower LGI1 binding than the remaining group (see Fig 3E). Thus, it appears that antibodies that compete with ADAM proteins for

antibodies. The amount of human antibodies bound to LGI1-Fc was not affected by the ADAMexHA application in this setting (AB060-110: 93  $\pm$  8%, mean  $\pm$  SD, of human IgG bound without ADAMexHA application; AB060-203: 100  $\pm$  10%). (E) Antibodies that interfere with ADAM22 binding to LGI1 have limited access to native LGI1. Relative quantification of the binding strength in hippocampal area CA3 of all human monoclonal LGI1 antibodies (mean  $\pm$  SEM) revealed higher mean fluorescent intensities (MFIs) for the non-ADAM22-competing group than for the ADAM22-competing group (unpaired *t* test, *p* < 0.0001, *n* = 7 and 17). Left: Example analysis with 2 antibodies. Human IgG is shown in red, nuclei (DAPI) in blue. Scale bar = 100 $\mu$ m. In the scatter plot, these examples are highlighted in red.



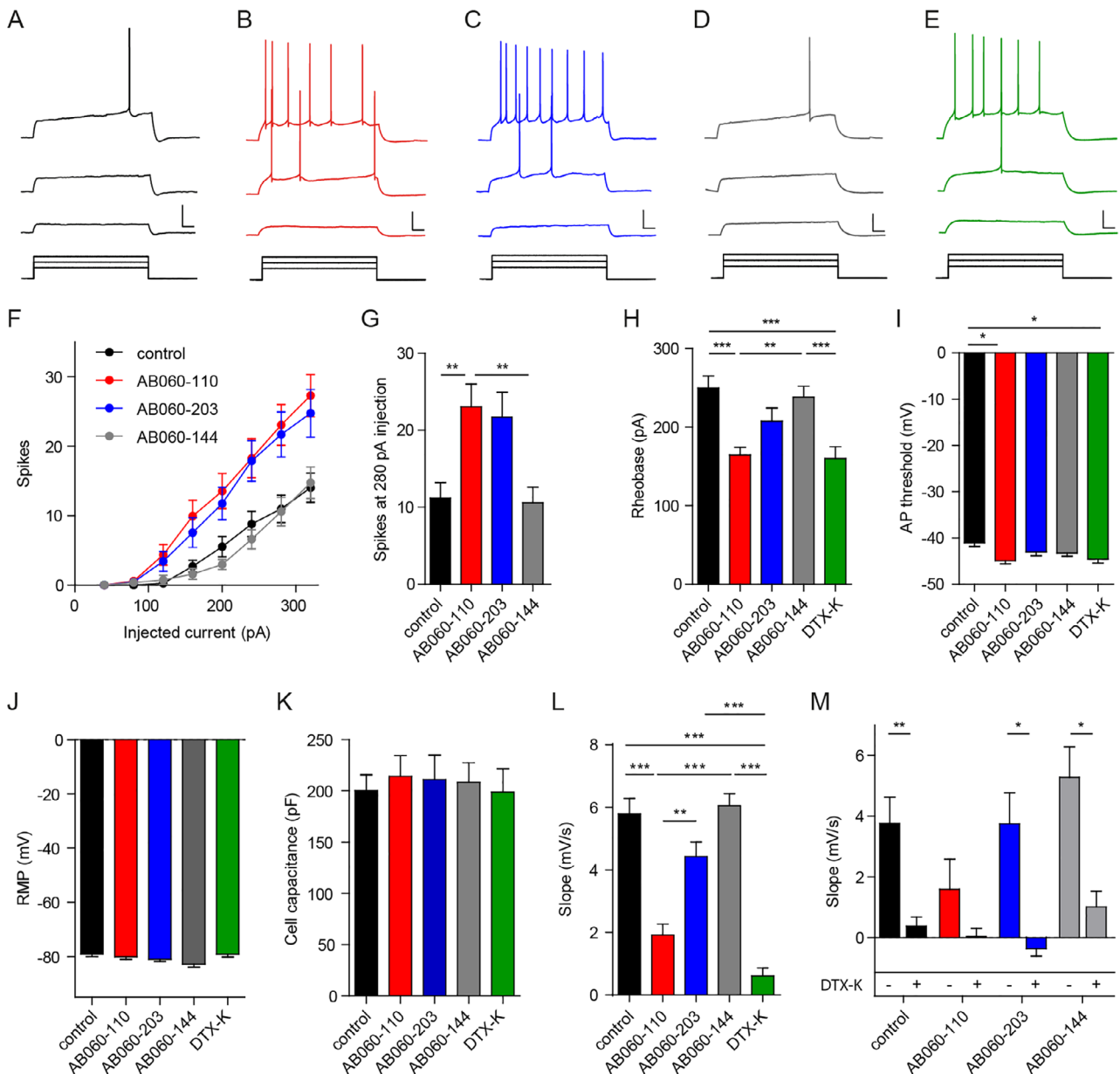


**FIGURE 5: AB060-110 and AB060-203 increased the excitability of CA3 pyramidal neurons in hippocampal slice cultures.** (A–E) Example traces of cell responses during depolarizing current steps (top: +160pA, middle: +120pA, bottom: +80pA) in CA3 pyramidal cells. Scale bars correspond to 20mV/160pA and 0.1 second. Slice cultures were left untreated (A), were treated with antibodies AB060-110 (B), AB060-203 (C), or AB060-144 (D), or were incubated with dendrotoxin-K (DTX-K; E). (F) Spike number/current intensity relationship displays a significant increase in spike number when slices were preincubated with AB060-110 or AB060-203. Two-way analysis of variance, control versus AB060-110: 200pA,  $p < 0.05$ ; 240pA,  $p < 0.01$ ; 280pA,  $p < 0.001$ ; 320pA,  $p < 0.001$ . Control versus AB060-203: 240pA,  $p < 0.01$ ; 280pA,  $p < 0.001$ ; 320pA,  $p < 0.001$ . Control versus AB060-144: not significant (n.s.). AB060-110 versus AB060-203: n.s. AB060-144 versus AB060-110: 160pA,  $p < 0.05$ ; 200pA,  $p < 0.001$ ; 240pA,  $p < 0.001$ ; 280pA,  $p < 0.001$ ; 320pA,  $p < 0.001$ . AB060-203 versus AB060-144: 200pA,  $p < 0.01$ ; 240pA,  $p < 0.001$ ; 280pA,  $p < 0.001$ ; 320pA,  $p < 0.001$ . (G) The number of spikes that were elicited by 280pA current injection was significantly higher in AB060-110-treated slices. ANOVA:  $p = 0.0011$ . (H) The rheobase was significantly reduced in cells that were preincubated with AB060-110 or with DTX-K. ANOVA:  $p < 0.0001$ . (I) The action potential (AP) threshold was significantly reduced in cells that were preincubated with AB060-110 or DTX-K. ANOVA:  $p = 0.0151$ . (J, K) The resting membrane potential (RMP; J) and the whole cell capacitance (K) were not altered in the different treatment conditions. Number of cells (F–K): control,  $n = 37$ ; AB060-110,  $n = 36$ ; AB060-203,  $n = 38$ ; AB060-144,  $n = 37$ ; DTX-K,  $n = 33$ . (L) The slope of the slowly depolarizing ramp at subthreshold stimulation intensities was significantly reduced in cells that were preincubated with AB060-110 or DTX-K. ANOVA:  $p < 0.0001$ . Control,  $n = 39$ ; AB060-110,  $n = 39$ ; AB060-203,  $n = 38$ ; AB060-144,  $n = 37$ ; DTX-K,  $n = 32$ . (M) Acute wash-in of 100nM DTX-K reduced the slope of the depolarizing ramp in control, AB060-203, and in AB060-144 conditions, (Figure legend continues on next page.)

binding to LGI1 have limited access to their targets in native tissue or reach their targets only after long exposure times, for example, upon turnover of ADAM-LGI1 complexes. Previous studies suggested that ADAM-competing and ADAM-noncompeting LGI1 antibodies bind to different domains in LGI1.<sup>31</sup> Expression of chimeric LGI1/3 and LGI1/2 constructs (Fig 4) revealed that AB060-110 selectively recognized the LRR domain of LGI1. In contrast, AB060-203 primarily bound to the EPTP repeat domain that mediates interactions of LGI1 with ADAM family proteins<sup>14</sup> and, weakly, to the LRR domain of LGI1 (see Fig 4). Taken together, AB060-203 targeted the EPTP repeat domain of LGI1, competed with ADAM22 binding, and showed reduced binding to native LGI1. In contrast, AB060-110 bound to the LRR domain of LGI1 and appeared to be much less affected by ADAM22, predicting efficient access of this antibody to LGI1-ADAM complexes *in vivo*.

#### **Human Monoclonal LGI1 Antibodies Elicit Increased Intrinsic Excitability and Synaptic Transmission of Hippocampal CA3 Neurons**

*Lgi1* mutations cause ADPEAF in humans, and targeted deletion of *Lgi1* in mice resulted in lethal myoclonic epileptic seizures.<sup>18–20</sup> The intrinsic excitability of CA3 neurons in hippocampal slice cultures was decreased by recombinant LGI1 and increased by genetic deletion of *Lgi1*.<sup>21</sup> Furthermore, acute application of IgG preparations from the sera of limbic encephalitis patients, potentially containing LGI1 antibodies, enhanced the excitability of CA3 pyramidal neurons in hippocampal slices.<sup>22</sup> Given the known link between CA3 excitability and seizure generation, we wanted to test whether these effects can be caused by LGI1 antibodies from the CSF of limbic encephalitis patients. Hippocampal slice cultures were treated with purified recombinant human IgG1 antibody AB060-110, AB060-203, or AB060-144 as a non-LGI1-reactive control (see Fig 1P, Q) for 24 to 48 hours, and the intrinsic excitability of CA3 pyramidal cells was examined (Fig 5). Patch clamp recordings were performed to determine the cells' excitability by injecting depolarizing currents (1 second, 40pA increment) under current clamp configuration and counting the numbers of generated APs. Treatment with AB060-110 or AB060-203 robustly increased cell excitability, with decreases in rheobase and AP thresholds at more hyperpolarized membrane potentials. In contrast,

treatment with control antibody AB060-144 did not change cell excitability, rheobase, or AP threshold. The effects of AB060-110 were more pronounced than the effects of AB060-203, in accord with their differences in epitope access (see Fig 3). Both resting membrane potential and capacitance of the CA3 cells were unchanged by antibody treatment (see Fig 5). *Lgi1* deletion has been shown to reduce the axonal density of Kv1.1/1.2 channels that limit glutamate release,<sup>21</sup> and we wondered whether LGI1 antibodies augmented neuronal excitability through this pathway also. The slowly depolarizing ramp elicited by subthreshold depolarization steps that represents a hallmark of the D-type potassium current<sup>36</sup> and is induced by Kv1 channels<sup>37</sup> was efficiently reduced by AB060-110, mimicking the effect of DTX-K, a selective antagonist of Kv1.1-containing potassium channels. As expected,<sup>21,38</sup> DTX-K increased the intrinsic cellular excitability of CA3 cells as well, similar to AB060-110. Furthermore, although an acute wash-in of DTX-K significantly reduced Kv1 currents in CA3 cells that had been treated with control antibody AB060-144 for 24 hours, the effect of DTX-K was occluded by prior treatment with LGI1 antibody AB060-110. These data indicate that LGI1 antibodies increase the intrinsic excitability of CA3 cells by reducing Kv1 currents.

We next set out to test whether LGI1 antibodies elicited AP-independent changes in synapses on CA3 cells as well. Application of LGI1 antibodies to hippocampal slice cultures for 24 hours significantly increased the amplitudes and the frequency (significantly different in the cumulative frequency distribution of the IELs) of AMPAR mEPSCs (Fig 6). As in the measurements of the intrinsic cellular excitability, LGI1 antibody AB060-203 elicited a smaller effect than AB060-110, but showed the same tendency. Treatment of hippocampal slice cultures with DTX-K for 24 hours shifted the mEPSC distribution to higher amplitudes as well. Thus, LGI1 antibodies increased cellular excitability and synaptic transmission of CA3 neurons, and both effects may be explained by a downregulation of axonal Kv1 currents.

Together, these data show that the addition of single patient-derived monoclonal antibodies was sufficient to interfere with LGI1 function that may be causal for LGI1 encephalitis symptoms. In addition, the profound effects of AB060-110 demonstrate that LGI1 antibodies can elicit hyperexcitability without direct interference with LGI1-ADAM interactions.

---

whereas treatment with AB060-110 occluded the reduction of the D-current by DTX-K. Paired *t* test with Bonferroni multiple comparison correction before versus after DTX-K: control,  $p = 0.0064$ ; AB060-110,  $p = 0.56$ ; AB060-203,  $p = 0.024$ ; AB060-144,  $p = 0.0104$ . Control,  $n = 8$ ; AB060-110,  $n = 8$ ; AB060-203,  $n = 9$ ; AB060-144,  $n = 7$ . Data is shown as mean with SEM. Dunn multiple comparison correction was performed in G-L. Significance levels: \* $p < 0.05$ ; \*\* $p < 0.01$ ; \*\*\* $p < 0.001$ .

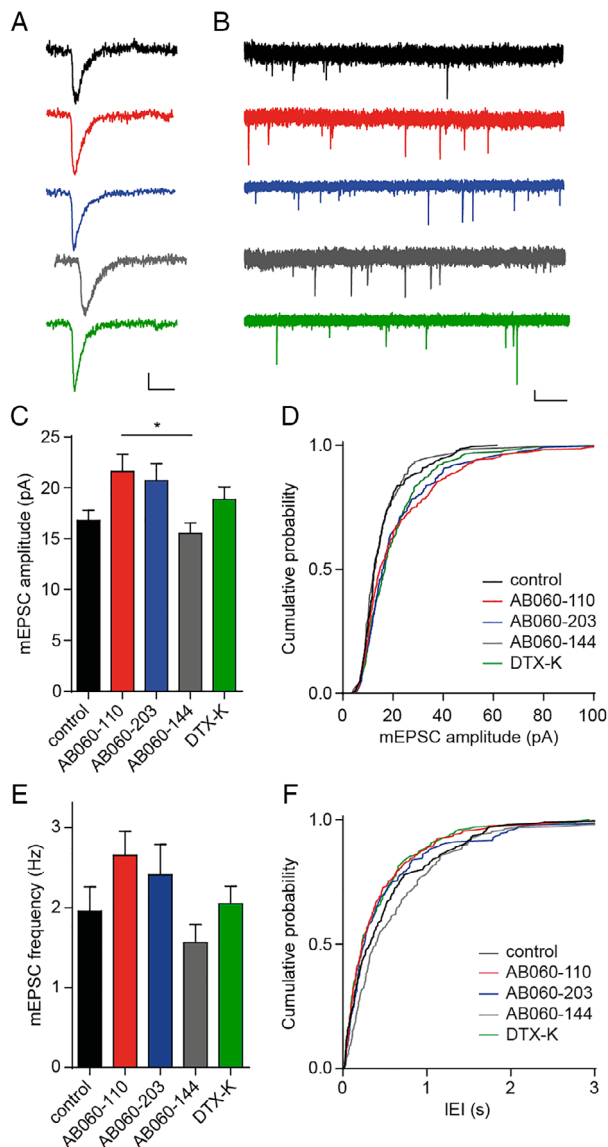


**FIGURE 6: AB060-110 and AB060-203 increased  $\alpha$ -amino-3-hydroxy-5-methyl-4-isoxazolepropionic acid receptor miniature excitatory postsynaptic currents in CA3 pyramidal neurons in hippocampal slice cultures.** (A) Example traces of miniature events recorded from CA3 cells in the presence of tetrodotoxin, gabazine, and D-AP5. Scale bar corresponds to 5 pA and 10 milliseconds. (B) Sample traces of miniature excitatory postsynaptic currents (mEPSCs). Scale bar corresponds to 10 pA and 500 milliseconds. (C) The mean amplitude of mEPSCs was significantly larger after 24-hour incubation with LGI1 antibody AB060-110 than after incubation with control antibody AB060-144. ANOVA:  $p = 0.0111$ . DTX-K = dendrotoxin-K. (D) Cumulative frequency distribution of mEPSC amplitudes was shifted to the right, indicating larger mEPSC amplitudes after incubation with LGI1 antibodies as compared to control antibody AB060-144. Control versus AB060-110:  $p = 0.0042$ ; control versus AB060-203:  $p = 0.003$ ; control versus AB060-144:  $p = 1$ ; control versus DTX-K:  $p = 0.0006$ ; AB060-144 versus AB060-110:  $p = 0.003$ ; AB060-144 versus AB060-203:  $p = 0.0042$ . (E) The mean mEPSC frequency was not changed significantly by LGI1 antibodies. ANOVA:  $p = 0.109$ . (F) Cumulative frequency distribution of mEPSC

(Figure legend continues on next column.)

## Discussion

Here, we provide insight into the antibody repertoire in the brain of LGI1 encephalitis patients by sequencing and cloning immunoglobulins expressed in CSF B cells and ASCs. A previous analysis of the antibody repertoire in NMDA receptor encephalitis revealed that only a small fraction of antibodies expressed by ASCs were directed to the NMDA receptor, and the majority of non-NMDA receptor-reactive antibodies targeted other brain epitopes.<sup>25</sup> Furthermore, the number of somatic hypermutations in the V genes of NMDA receptor autoantibodies among all patients was significantly lower compared to CSF antibodies not targeting the NMDA receptor of the same patients.<sup>25</sup> The NMDA receptor encephalitis repertoire contained antibodies lacking any mutation as compared to the germline sequence.<sup>25,30</sup> Our findings in LGI1 encephalitis are in striking contrast. First, in LGI1 encephalitis, the fraction of ASCs expressing LGI1 antibodies was high. Second, reactions to brain antigens other than LGI1 were rare. Third, the V gene sequences for the heavy and light chains of the LGI1 antibodies contained many mutations as compared to the germline sequence, particularly in Patient AIE054. Together with the finding that LGI1 encephalitis but not NMDA receptor encephalitis is strongly associated with specific human leukocyte antigen haplotypes,<sup>10–13</sup> these data indicate fundamental differences between the 2 most common AIEs. They may represent an immunological basis reflecting the clinical diversity between the 2 diseases, including not only etiology, age and gender preferences, and tumor associations, but also clinical courses and treatment responses.

Patients with LGI1 encephalitis, like the patients examined here, frequently have normal CSF cell counts and protein levels and no oligoclonal IgG bands. The presence of LGI1 antibody-producing cells in the CSF of all 3 investigated CSF samples in this study, although only 1 of them had oligoclonal IgG bands and only 1 other had LGI1 antibody detectable in routine cell-based assays, proves that these patients also have an intrathecal LGI1 autoantibody production. Antibodies against brain targets

intervent intervals (IEIs) was shifted to the left, indicating shorter intervals after incubation with LGI1 antibodies as compared to control antibody AB060-144. Control versus AB060-110:  $p = 1$ ; control versus AB060-203:  $p = 1$ ; control versus AB060-144:  $p = 0.4242$ ; control versus DTX-K:  $p = 1$ ; AB060-144 versus AB060-110:  $p = 0.0054$ ; AB060-144 versus AB060-203:  $p = 0.0294$ . Number of cells: control,  $n = 23$ ; AB060-110,  $n = 21$ ; AB060-203,  $n = 20$ ; AB060-144,  $n = 21$ ; DTX-K,  $n = 20$ . Data is shown as mean + SEM (C,E). Dunn multiple comparison correction was performed in C, E; Kolmogorov-Smirnov test with Bonferroni multiple comparison correction was performed in D, F. Significance levels: \* $p < 0.05$ ; \*\* $p < 0.01$ ; \*\*\* $p < 0.001$ .

TABLE. Patient Characteristics

AIE	Age, yr/Sex	Tumor	Leading Clinical Symptoms	MRI	Time from Onset, wk	Previous Immunotherapy	AEDs	Ab Titer	CSF: cells/ $\mu$ l; protein, mg/l; mg/l; OCB
054	71/F	Neuroendocrine intestinal tumor	FBDS, anterograde amnesia, focal seizures	Bilateral mesiotemporal swelling	36	MP, Pred, IA, MTX	Valproate, levetiracetam	1:100 (S), neg. (CSF)	2; 344; neg.
060	63/M	No	Confusion, behavioral changes, sopor, myoclonus	Left > right mesiotemporal hyperintensity	22	MP, IA, IVIG	Valproate, oxazepam	1:320 (S), pos. (CSF)	5; 468; neg.
137	74/M	No	FBDS	Left mesiotemporal hyperintensity, mild subcortical atrophy	10	Pred	Eslicarbazepine	1:320 (S), neg. (CSF)	0; 409; pos.

The patients show typical features of LGI1 encephalitis, such as older age, mesiotemporal MRI changes, and noninflammatory CSF.  
 Ab = antibody; AED = antiepileptic drug; AIE = autoimmune encephalopathy; CSF = cerebrospinal fluid; F = female; FBDS = faciobrachial dystonic seizures; IA = immunoadsorption; IVIG = intravenous immunoglobulins; M = male; MP = methylprednisolone; MRI = magnetic resonance imaging; MTX = methotrexate; neg. = negative; OCB = oligoclonal bands; pos. = positive; Pred = prednisolone; S = serum.

may escape detection within the CSF, as they quickly bind to their antigens.<sup>39</sup> This raises the question of whether intense immunotherapy may be required also in patients with low-level antibodies and a compatible clinical picture and, even more intriguing, whether undetectable levels in routine assays may still account for slowly progressing cognitive decline in a small fraction of patients with atypical dementia, given that cases with LGI1 antibody-associated dementia are increasingly reported.<sup>40,41</sup>

Hippocampal CA3 neurons are a frequent focus of seizure generation, and their intrinsic excitability was increased by genetic deletion of *Lgi1* through downregulation of axonal Kv1 potassium channels.<sup>21</sup> Kv1 channel inactivation at the axon initial segment is known to result in AP broadening, increased synaptic strength, and neuronal hyperexcitability.<sup>38,42,43</sup> We show that isolated recombinant LGI1 antibodies increase the intrinsic excitability of hippocampal CA3 neurons by reducing Kv1 currents as well. This finding supports the view that antibodies are directly pathogenic in LGI1 encephalitis. The antibody-induced neuronal overexcitation may explain seizure symptoms in LGI1 encephalitis, including FBDS and focal and generalized seizures, which are often followed by cognitive impairment if not sufficiently treated with immunosuppression.<sup>44</sup> Also, we show an LGI1 antibody-elicited increase in AMPAR mEPSC amplitude and frequency in CA3 neurons of hippocampal

slice cultures that may rely on reduced Kv1 currents as well. Together, LGI1 antibodies increase intrinsic cellular excitability and glutamatergic transmission, and both effects may contribute to seizure generation in LGI1 encephalitis. Stereotactic injection of human CSF containing LGI1 antibodies into the dorsal hippocampus of mice increased the probability of glutamate release at CA3–CA1 synapses, but did not alter the intrinsic excitability of CA1 cells.<sup>24</sup> CA1 pyramidal neurons may be less sensitive to LGI1 antibodies than CA3 neurons due to their low level of Kv1.1.<sup>45,46</sup>

Targeted deletion of *Lgi1* altered AMPAR-mediated synaptic transmission in CA1 neurons. Increased mEPSC amplitudes were detected in acute slices of *Lgi1* null mice at P8/9, in line with a stronger glutamatergic drive onto CA1 neurons.<sup>47</sup> In contrast, in acute hippocampal slices of P14/15 mice lacking *Lgi1*, decreased mEPSC amplitudes and a reduced AMPA/NMDA ratio indicated postsynaptic effects.<sup>19</sup> Similar results were observed in CA1 or dentate gyrus granule cells from cultured hippocampal slices prepared from *Lgi1* null mice at P6–8 before seizure onset.<sup>16</sup> The reason for these discrepancies is not known, but additional experiments indicated that LGI1 promotes postsynaptic maturation through ADAM22 and PSD-95.<sup>16</sup> Antibody-mediated interference with the LGI1–ADAM22–PSD-95 link is expected to alter the composition of the postsynaptic density as well. This might result

in deficient AMPAR recruitment<sup>14,16,23,31</sup> and underlie cognitive deficits in LGI1 encephalitis. It is possible that the inhibitory effects of LGI1 antibodies are limited by the accessibility of mature synaptic structures and are detected only after long exposition times.

Because several unavoidable autoreactive in vivo mechanisms, such as complement activation and inflammatory processes, are not active in slice cultures, the observed effects of LGI1 antibodies AB060-110 and AB060-203 are most likely mediated by direct binding to their respective epitopes. It was reported that sera of patients with LGI1 encephalitis cause LGI1-ADAM22 complex internalization in transfected HEK293T cells,<sup>44</sup> suggesting downregulation of LGI1-ADAM22 complexes as a pathogenic mechanism of LGI1 antibodies. The same mechanism that autoantibodies extracellularly bind to target proteins and cause their selective internalization was reported for autoantibodies to NMDA receptors<sup>48</sup> and to AMPARs.<sup>49</sup> In contrast, recent structural analyses revealed higher-order LGI1-ADAM complexes with 2:2 or 3:3 configurations.<sup>15</sup> LGI1 antibodies like AB060-110 may interfere with LRR domain interactions and thereby destabilize these complexes. Other LGI1 antibodies like AB060-203 are thought to prevent or disrupt LGI1-ADAM interactions. Given that ADAM22/23 in *Lgi1* knockout mouse brain was delocalized from synaptic fractions,<sup>19</sup> ADAM22/23 unbound from LGI1 due to LGI1 antibodies might be rapidly internalized from synaptic membranes. Thus, irrespective of the target epitope and their direct mode of action, LGI1 antibodies may elicit a reduction in the number of LGI1-ADAM complexes from synaptic membranes. Antibodies targeting different LGI1 epitopes may act in synergy in patients' CSF. In any case, the functional effects of monoclonal LGI1 antibodies demonstrated here indicate direct pathogenicity in LGI1 encephalitis and provide the rationale for clinicians for sufficiently "aggressive" immunotherapy and second-line or prolonged treatment in relapsing or slowly progressing cases.

Although immunotherapy is fast and efficient in some LGI1 encephalitis patients, other cases are characterized by a long and continuously progressing disease process, including memory deficits, apathy, and difficulties with spatial orientation.<sup>4</sup> Recent studies indicated that a high CSF index and specific IgG isotypes might be predictive of refractory symptoms and cognitive impairment.<sup>9,44</sup> In a patient with a long-lasting progressive LGI1 encephalitis (AIE060), our screen detected LGI1 antibodies of IgG1, IgG2, and IgG4 subtype in CSF ASCs and MBCs. In contrast, in Patient AIE054, we found exclusively antibodies of IgG2 isotype in ASCs. It should be examined in larger cohorts whether the presence of IgG1 or IgG4 antibodies is predictive of cases with severe, long-lasting

disease courses. The monoclonal antibodies described here will be helpful in testing these and other hypotheses and in developing refined diagnostics.

## Acknowledgment

This study was supported by the German Research Foundation (SFB 958, 1315, FOR 3004, SPP 1665, Exc 257 to D.S.; PR 1274/2-1, PR 1274/3-1 to H.P.), Helmholtz Association (Helmholtz ExNet-0009-Phase 2-3 NeuroCure to D.S.), Federal Ministry of Education and Research (SMARTAGE 01GQ1420A to D.S.), Charité Foundation to D.S., JSPS/MEXT KAKENHI (19H03331 to Y.F.; 17H03678, 19K22548 to M.F.), Hori Sciences and Arts Foundation to M.F., Japan Epilepsy Research Foundation to Y.F., and Daiko Foundation to Y.F.

We thank D. Brandl, S. Stadler, P. Loge, and S. Rieckmann for excellent technical assistance, T. Frey for characterization of GluN1-ATD-Fc, J. Schlender for help with stainings, B. Rost for help with slice cultures, and R. Murugan for advice.

## Author Contributions

H.-C.K., M.F., H.P., and D.S. contributed to the conception and design of the study; H.-C.K., J.K., A.S., Y.F., D.P., R.P.S., B.I., S.K., A.B.K., and M.F. contributed to the acquisition and analysis of data; H.-C.K., J.K., A.S., and H.P. contributed to drafting the text and preparing the figures.

## Potential Conflicts of Interest

Nothing to report.

## References

- Irani SR, Alexander S, Waters P, et al. Antibodies to Kv1 potassium channel-complex proteins leucine-rich, glioma inactivated 1 protein and contactin-associated protein-2 in limbic encephalitis, Morvan's syndrome and acquired neuromyotonia. *Brain* 2010;133:2734–2748.
- Lai M, Huijbers MG, Lancaster E, et al. Investigation of LGI1 as the antigen in limbic encephalitis previously attributed to potassium channels: a case series. *Lancet Neurol* 2010;9:776–785.
- Dalmau J, Geis C, Graus F. Autoantibodies to synaptic receptors and neuronal cell surface proteins in autoimmune diseases of the central nervous system. *Physiol Rev* 2017;97:839–887.
- van Sonderen A, Petit-Pedrol M, Dalmau J, et al. The value of LGI1, Caspr2 and voltage-gated potassium channel antibodies in encephalitis. *Nat Rev Neurol* 2017;13:290–301.
- Crisp SJ, Kullmann DM, Vincent A. Autoimmune synaptopathies. *Nat Rev Neurosci* 2016;17:103–117.
- Dalmau J, Graus F. Antibody-mediated encephalitis. *N Engl J Med* 2018;378:840–851.
- Irani SR, Michell AW, Lang B, et al. Faciobrachial dystonic seizures precede Lgi1 antibody limbic encephalitis. *Ann Neurol* 2011;69:892–900.



8. Finke C, Pruss H, Heine J, et al. Evaluation of cognitive deficits and structural hippocampal damage in encephalitis with leucine-rich, glioma-inactivated 1 antibodies. *JAMA Neurol* 2017;74:50–59.
9. Gadoth A, Zekeridou A, Klein CJ, et al. Elevated LGI1-IgG CSF index predicts worse neurological outcome. *Ann Clin Transl Neurol* 2018;5: 646–650.
10. Binks S, Varley J, Lee W, et al. Distinct HLA associations of LGI1 and CASPR2-antibody diseases. *Brain* 2018;141:2263–2271.
11. Kim TJ, Lee ST, Moon J, et al. Anti-LGI1 encephalitis is associated with unique HLA subtypes. *Ann Neurol* 2017;81:183–192.
12. van Sonderen A, Roelen DL, Stoop JA, et al. Anti-LGI1 encephalitis is strongly associated with HLA-DR7 and HLA-DRB4. *Ann Neurol* 2017;81:193–198.
13. Mueller SH, Farber A, Pruss H, et al. Genetic predisposition in anti-LGI1 and anti-NMDA receptor encephalitis. *Ann Neurol* 2018;83:863–869.
14. Fukata Y, Adesnik H, Iwanaga T, et al. Epilepsy-related ligand/receptor complex LGI1 and ADAM22 regulate synaptic transmission. *Science* 2006;313:1792–1795.
15. Yamagata A, Miyazaki Y, Yokoi N, et al. Structural basis of epilepsy-related ligand-receptor complex LGI1-ADAM22. *Nat Commun* 2018; 9:1546.
16. Lovero KL, Fukata Y, Granger AJ, et al. The LGI1-ADAM22 protein complex directs synapse maturation through regulation of PSD-95 function. *Proc Natl Acad Sci U S A* 2015;112:E4129–E4137.
17. Schulte U, Thumfart JO, Klocker N, et al. The epilepsy-linked Lgi1 protein assembles into presynaptic Kv1 channels and inhibits inactivation by Kvbeta1. *Neuron* 2006;49:697–706.
18. Yu YE, Wen L, Silva J, et al. Lgi1 null mutant mice exhibit myoclonic seizures and CA1 neuronal hyperexcitability. *Hum Mol Genet* 2010; 19:1702–1711.
19. Fukata Y, Lovero KL, Iwanaga T, et al. Disruption of LGI1-linked synaptic complex causes abnormal synaptic transmission and epilepsy. *Proc Natl Acad Sci U S A* 2010;107:3799–3804.
20. Chabrol E, Navarro V, Provenzano G, et al. Electroclinical characterization of epileptic seizures in leucine-rich, glioma-inactivated 1-deficient mice. *Brain* 2010;133:2749–2762.
21. Seagar M, Russier M, Caillard O, et al. LGI1 tunes intrinsic excitability by regulating the density of axonal Kv1 channels. *Proc Natl Acad Sci U S A* 2017;114:7719–7724.
22. Lalic T, Pettingill P, Vincent A, et al. Human limbic encephalitis serum enhances hippocampal mossy fiber-CA3 pyramidal cell synaptic transmission. *Epilepsia* 2011;52:121–131.
23. Petit-Pedrol M, Sell J, Planaguma J, et al. LGI1 antibodies alter Kv1.1 and AMPA receptors changing synaptic excitability, plasticity and memory. *Brain* 2018;141:3144–3159.
24. Romoli M, Krashia P, Sen A, et al. Hippocampal epileptogenesis in autoimmune encephalitis. *Ann Clin Transl Neurol* 2019;6:2261–2269.
25. Kreye J, Wenke NK, Chayka M, et al. Human cerebrospinal fluid monoclonal N-methyl-D-aspartate receptor autoantibodies are sufficient for encephalitis pathogenesis. *Brain* 2016;139:2641–2652.
26. Malviya M, Barman S, Golombeck KS, et al. NMDAR encephalitis: passive transfer from man to mouse by a recombinant antibody. *Ann Clin Transl Neurol* 2017;4:768–783.
27. Tiller T, Meffre E, Yurasov S, et al. Efficient generation of monoclonal antibodies from single human B cells by single cell RT-PCR and expression vector cloning. *J Immunol Methods* 2008;329:112–124.
28. Wardemann H, Yurasov S, Schaefer A, et al. Predominant autoantibody production by early human B cell precursors. *Science* 2003; 301:1374–1377.
29. Murugan R, Buchauer L, Triller G, et al. Clonal selection drives protective memory B cell responses in controlled human malaria infection. *Sci Immunol* 2018;3. pii: eaap8029.
30. Wenke NK, Kreye J, Andrzejak E, et al. N-methyl-D-aspartate receptor dysfunction by unmutated human antibodies against the NR1 subunit. *Ann Neurol* 2019;85:771–776.
31. Ohkawa T, Fukata Y, Yamasaki M, et al. Autoantibodies to epilepsy-related LGI1 in limbic encephalitis neutralize LGI1-ADAM22 interaction and reduce synaptic AMPA receptors. *J Neurosci* 2013;33: 18161–18174.
32. Rost BR, Schneider F, Grauel MK, et al. Optogenetic acidification of synaptic vesicles and lysosomes. *Nat Neurosci* 2015;18:1845–1852.
33. Gray D. A role for antigen in the maintenance of immunological memory. *Nat Rev Immunol* 2002;2:60–65.
34. Arino H, Armangue T, Petit-Pedrol M, et al. Anti-LGI1-associated cognitive impairment: presentation and long-term outcome. *Neurology* 2016;87:759–765.
35. Irani SR, Pettingill P, Kleopa KA, et al. Morvan syndrome: clinical and serological observations in 29 cases. *Ann Neurol* 2012;72:241–255.
36. Storm JF. Temporal integration by a slowly inactivating K<sup>+</sup> current in hippocampal neurons. *Nature* 1988;336:379–381.
37. Metz AE, Spruston N, Martina M. Dendritic D-type potassium currents inhibit the spike afterdepolarization in rat hippocampal CA1 pyramidal neurons. *J Physiol* 2007;581:175–187.
38. Bekkers JM, Delaney AJ. Modulation of excitability by alpha-dendrotoxin-sensitive potassium channels in neocortical pyramidal neurons. *J Neurosci* 2001;21:6553–6560.
39. Castillo-Gomez E, Kastner A, Steiner J, et al. The brain as immunoprecipitator of serum autoantibodies against N-methyl-D-aspartate receptor subunit NR1. *Ann Neurol* 2016;79:144–151.
40. Marquetand J, van Lessen M, Bender B, et al. Slowly progressive LGI1 encephalitis with isolated late-onset cognitive dysfunction: a treatable mimic of Alzheimer's disease. *Eur J Neurol* 2016;23: e28–e29.
41. Reintjes W, Romijn MD, Hollander D, et al. Reversible dementia: two nursing home patients with voltage-gated potassium channel antibody-associated limbic encephalitis. *J Am Med Dir Assoc* 2015; 16:790–794.
42. Geiger JR, Jonas P. Dynamic control of presynaptic Ca<sup>2+</sup> inflow by fast-inactivating K<sup>(+)</sup> channels in hippocampal mossy fiber boutons. *Neuron* 2000;28:927–939.
43. Kole MH, Letzkus JJ, Stuart GJ. Axon initial segment Kv1 channels control axonal action potential waveform and synaptic efficacy. *Neuron* 2007;55:633–647.
44. Thompson J, Bi M, Murchison AG, et al. The importance of early immunotherapy in patients with faciobrachial dystonic seizures. *Brain* 2018;141:348–356.
45. Kues WA, Wunder F. Heterogeneous expression patterns of mammalian potassium channel genes in developing and adult rat brain. *Eur J Neurosci* 1992;4:1296–1308.
46. Rhodes KJ, Strassle BW, Monaghan MM, et al. Association and colocalization of the Kvbeta1 and Kvbeta2 beta-subunits with Kv1 alpha-subunits in mammalian brain K<sup>+</sup> channel complexes. *J Neurosci* 1997;17:8246–8258.
47. Boillot M, Lee CY, Allene C, et al. LGI1 acts presynaptically to regulate excitatory synaptic transmission during early postnatal development. *Sci Rep* 2016;6:21769.
48. Hughes EG, Peng X, Gleichman AJ, et al. Cellular and synaptic mechanisms of anti-NMDA receptor encephalitis. *J Neurosci* 2010; 30:5866–5875.
49. Lai M, Hughes EG, Peng X, et al. AMPA receptor antibodies in limbic encephalitis alter synaptic receptor location. *Ann Neurol* 2009;65: 424–434.